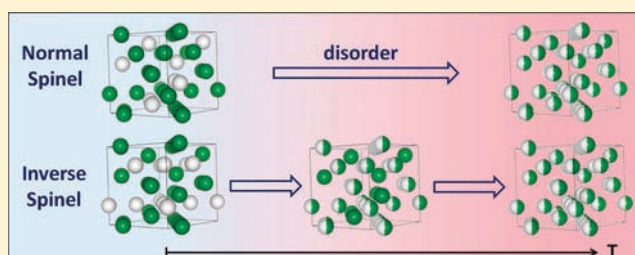


Universal Electrostatic Origin of Cation Ordering in A_2BO_4 Spinel Oxides

Vladan Stevanović,* Mayeul d’Avezac, and Alex Zunger

National Renewable Energy Laboratory, Golden, Colorado 80401, United States

ABSTRACT: The crystal structures of A_2BO_4 spinel oxides are classified as either normal or inverse, representing different distributions of the A and B cations over the tetrahedrally and octahedrally coordinated cation sites. These structures undergo characteristic structural changes as a function of temperature: (i) the nominally disordered inverse structure orders crystallographically at low T , and (ii) at finite temperatures, both inverse and normal develop characteristic distributions of cations associated with order–disorder structural changes. We show here that all of these universal features emerge naturally from a simple point-ion electrostatic (PIE) model with a single adjustable parameter. Monte Carlo simulations of the PIE Hamiltonian provide quantitative order–disorder characteristic temperatures. We show that, with the help of the PIE model, the magnitude of the temperatures can be inferred from the nominal charges of the atomic species in the spinel. Indeed, we show that characteristic order-disorder temperatures in 3-2 spinels (nominal charges $Z_A = 3$ and $Z_B = 2$) are approximately an order of magnitude lower than in 2-4 spinels, thus explaining why typical 3-2 samples exhibit much larger degrees of disorder than those belonging to the 2-4 class.



INTRODUCTION

The A_2BO_4 spinel oxides¹ form a family of ~ 120 compounds² spanning a significant range of properties including both ferro- and antiferromagnetism,³ coexistence of transparency and conductivity,⁴ superconductivity,⁵ and ferroelectricity.⁶ In the spinel structure the A and B metal atoms are distributed over the interstitial sites of a distorted face-centered cubic (fcc) oxygen sublattice. Half of the octahedrally coordinated fcc sites (O_h) and an eighth of the tetrahedrally coordinated interstitials (T_d) are populated by the A and B cations. It is convenient to introduce the degree of inversion λ , a dimensionless quantity describing relative concentration of the A cations on T_d sites. In terms of λ the spinel chemical formula can be written as $[A_{2-\lambda}B_\lambda](A_\lambda B_{1-\lambda})O_4$, with brackets and parentheses representing the O_h and T_d sites, respectively. Depending on the λ value, spinels are sorted in two main categories: (i) normal ($\lambda = 0$) spinels, an ordered phase with cubic ($Fd\bar{3}m$) symmetry having the O_h sites occupied exclusively by A cations and the T_d sites by B cations, as shown in Figure 1a; and (ii) inverse ($\lambda = 1$) spinels, having half the A cations occupying the T_d sites and the other half of A together with all of the B atoms populating the O_h sites, much as in a 50%–50% binary alloy on O_h sites. Therefore, inverse spinel corresponds to a class of configurations rather than a single crystallographic structure. In such cases one expects ordering at low temperatures. Indeed, tetragonal $P4_122$ ordering (see Figure 1b) has been observed experimentally in Mg_2TiO_4 ,^{7–9} Zn_2TiO_4 , Mn_2TiO_4 ,^{9–11} and Fe_2NiO_4 ,¹² inverse spinels. Theoretical ab initio case-by-case studies also predict this type of ordering in Ga_2MgO_4 , In_2MgO_4 , Mg_2SnO_4 , Zn_2SnO_4 ,

Zn_2TiO_4 ,^{13,14} and Fe_2MgO_4 , Al_2NiO_4 , Fe_3O_4 inverse spinel oxides.¹⁵ Structures with $0 < \lambda < 1$, to which we refer as dual spinels, are also possible. However, they are the high-temperature structures (disordered-dual) and it is known that the true ground-state structure in spinels is either normal or inverse.¹⁶

The normal and ordered-inverse structures are also known to undergo characteristic structural changes as a function of temperature,^{8,13,14,16} which are a consequence of the A and B cations exchanging their lattice sites as shown schematically in Figure 2. In normal spinels, what happens is a continuous increase in disorder, also known as nonconvergent disordering,¹⁷ which preserves the overall cubic ($Fd\bar{3}m$) symmetry and during which λ increases with temperature from zero to $\lambda = 0.67$, a state with maximal configurational entropy. In inverse spinels, on the other hand, two different structural changes are identified. Compounds that are known to order in the tetragonal $P4_122$ symmetry undergo a first-order transition to the disordered-inverse state with $\lambda = 1$ and cubic ($Fd\bar{3}m$) symmetry. Upon increasing temperature above the first-order transition, they start to disorder continuously to the disordered-dual state, with λ slowly decreasing to 0.67, while still retaining the overall cubic symmetry.

Previously, O’Neil and Navrotsky¹⁶ proposed an empirical model describing the behavior of λ with temperature. It is based on the observation that electrostatic interactions are likely to represent the largest contribution to the lattice energy. However, it makes the simplifying assumption that configurations for any λ are fully

Received: April 14, 2011

Published: June 24, 2011

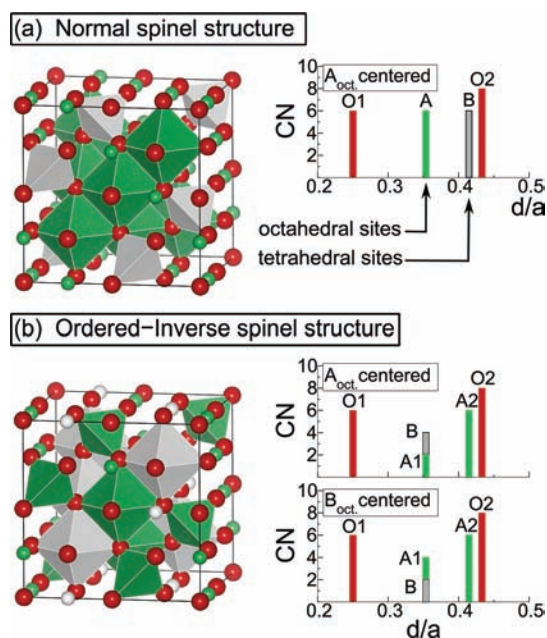


Figure 1. (a) Crystal structure of the normal A_2BO_4 spinel structure (left). Oxygen atoms are shown in red, A atoms in green, and B atoms in gray. The A and B atoms are shown together with their coordination octahedra and tetrahedra, respectively. In addition (on the right), the coordination number (CN) of the octahedrally coordinated cations as a function of the scaled distance is presented. (b) Same, but for the ordered-inverse ($P4_122$) spinel structure. In this case the CN of both octahedral A and octahedral B cations is shown.

random; that is, short-range order is completely neglected. As a result, the model captures only the continuous disordering behavior starting from normal spinels (left side of Figure 2) and randomly disordered inverse spinels (top-right of Figure 2).

We show in this paper that all of the universal order–disorder features in spinel oxides emerge naturally from a simple point-ion electrostatic (PIE) model, where the only adjustable parameter, the dielectric constant, is fitted to density functional theory (DFT) total energies. First, the model provides an explanation for the normal versus inverse structural preference in spinel oxides,¹⁸ a problem that dates back to the 1920s and the work of Barth and Posnjak.^{19,20} Second, the PIE model identifies the tetragonal $P4_122$ structure as the *universal* ground-state structure of inverse spinels. Third, Monte Carlo simulations of the PIE Hamiltonian, which naturally include the short-range order, provide an accurate description for the universal finite temperature behavior in these systems and also provide quantitative order–disorder characteristic temperatures.

POINT-ION ELECTROSTATIC MODEL

The electrostatic energy of a configuration σ of point charges Z_i located at the vertices \mathbf{R}_i of the spinel lattice is

$$E_{\text{PIE}}(\sigma) = \frac{1}{2\epsilon} \sum_{i,j} \frac{Z_i(\sigma)Z_j(\sigma)}{|\mathbf{R}_i - \mathbf{R}_j|} \quad (1)$$

where ϵ stands for the dielectric constant. We compute the sum in eq 1 using the Ewald summation formula,²¹ assuming the formal oxidation states as ionic charges (Z_A , Z_B , Z_O). In the cubic ($Fd3m$) spinel structure, positions of the cations are determined only by the lattice constant a while positions of

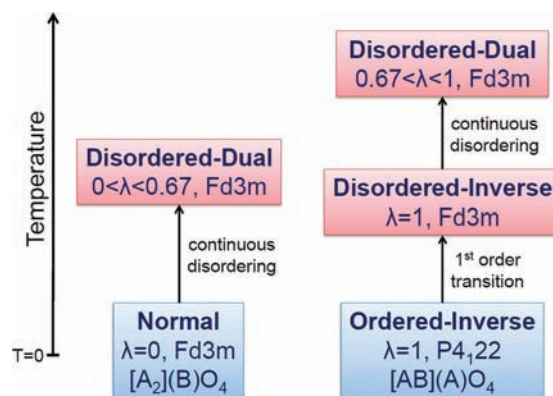


Figure 2. Flow diagram describing temperature dependence of cation distribution in spinel oxides. Two types of behaviors are identified across all spinel oxide materials, depending on whether a given material is normal or inverse at $T = 0$ K. In the former case, a continuous increase in disorder from the normal structure is found. In the latter case, inverse spinels undergo two structural changes with temperature: (i) first-order transition from ordered-inverse to disordered-inverse and (ii) continuous disordering from disordered-inverse to disordered-dual.

the oxygen atoms depend also on the dimensionless displacement parameter u . If one fixes $Z_O = -2$ and writes the cation charge located at the cations site i as $Z_i = [Z_A(1 + S_i)/2 + Z_B(1 - S_i)/2]$, where S_i is the “spin” variable that takes two values, either $S_i = +1$ (when $Z_i = Z_A$) or $S_i = -1$ (when $Z_i = Z_B$), then the electrostatic energy of any configuration σ can be written as the sum of three terms $E_{\text{PIE}} = E_1 + E_2 + E_3$, where

$$\begin{aligned} E_1 &= E_{\text{PIE}}(Z_{\text{oct}} = Z_{\text{tet}} = \bar{Z}) \\ E_2 &= \frac{1}{2} Z_r N [(2\lambda - 1)\phi_{\text{tet}} + (2 - 2\lambda)\phi_{\text{oct}}] \Big|_{Z_{\text{oct}} = Z_{\text{tet}} = \bar{Z}} \quad (2) \\ E_3 &= \frac{Z_r^2}{8a\epsilon} \sum_{i,j}^{\text{cations}} \frac{S_i(\sigma)S_j(\sigma)}{|\rho_i - \rho_j|} \end{aligned}$$

where λ is the degree of inversion (relative concentration of the A cations on T_d sites), N is the number of formula units in the unit cell, ϕ_{tet} and ϕ_{oct} are the electrostatic potentials of the corresponding cation sites, and \bar{Z} and Z_r are the average $[(Z_A + Z_B)/2]$ and relative $(Z_A - Z_B)$ cation charges, respectively. $\rho_i = \mathbf{R}_i/a$ are the scaled atomic positions. With Z_A and Z_B fixed, the E_1 term depends only on the structural parameters a and u and is simply the PIE energy with all cations having the same \bar{Z} charge. The E_2 term represents the weighted sum of the electrostatic energies $Z_r\phi_{\text{oct}}$ and $Z_r\phi_{\text{tet}}$ of the relative Z_r charge placed on both the octahedral and the tetrahedral site with all other cations having the \bar{Z} charge. This term depends on (a, u, λ) . The only term that depends explicitly on the actual configuration σ is the E_3 term, which represents the PIE energy of the lattice containing only cations (no anions) with virtual $Z_A = Z_r/2$ and $Z_B = -Z_r/2$ charges. It is important to note that, when taken individually, each of the three terms E_1 , E_2 , and E_3 in eq 2 corresponds to a fictitious system that is not charge-neutral. Their sum is naturally charge-neutral, as is the physical system. Each term can only be computed separately from the others through the introduction of a neutralizing background.

We now discuss the relative PIE energies between two different configurations σ_1 and σ_2 . In the case when σ_1 and σ_2

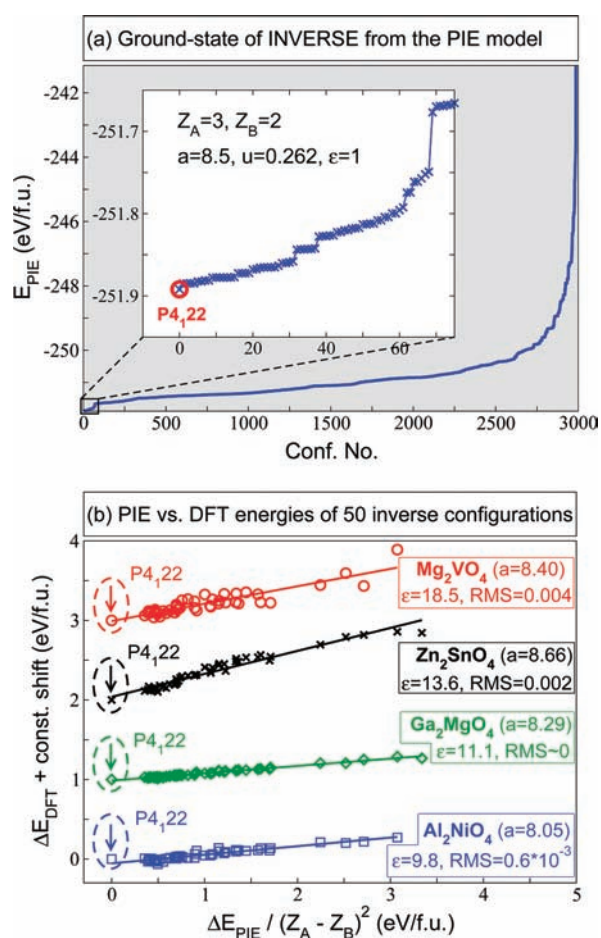


Figure 3. (a) PIE energies of all 2987 inverse configurations with 56 atoms or less. (b) Regression $\Delta E_{\text{DFT}} = 1/\epsilon \Delta E_{\text{PIE}}$ ($\epsilon = 1$) between the PIE and DFT energies calculated relative to the ordered ($P4_122$) inverse spinel structure for four different inverse spinel materials. a represents the experimental lattice constants (in angstroms). ϵ are the fitted PIE scaling factors. The rms are the root-mean-square errors of the fit.

correspond to configurations with the same λ value (e.g., $\lambda = 1$) their E_1 and E_2 terms have exactly the same value and the relative electrostatic energy equals the difference only between the E_3 terms, that is, $E_{\text{PIE}}(\sigma_1) - E_{\text{PIE}}(\sigma_2) = E_3(\sigma_1) - E_3(\sigma_2)$. Since the sum in E_3 runs only over cations, $\Delta E_3(\sigma_1, \sigma_2)$ does not depend at all on the oxygen displacement parameter u . In that case, $\Delta E_{\text{PIE}}(\sigma_1, \sigma_2)$ scales with the factor $Z_r^2/a\epsilon$, which, as will be shown later, determines the transition temperature for the first-order transition from ordered-inverse to disordered-inverse.

■ NORMAL VERSUS INVERSE STRUCTURE IN A_2BO_4 SPINELS

We have recently shown¹⁸ that the $T = 0$ normal versus inverse structural preference in A_2BO_4 spinel oxides can be described accurately using the PIE model. By comparison of the electrostatic energy of the normal spinel structure with those of inverse configurations, the PIE model leads to simple rules delineating normal from inverse spinels on the basis of the relative formal cation charges Z_A versus Z_B and the geometric anion displacement parameter u , which describes the asymmetry between the A–O and B–O bonds. If $Z_A > Z_B$, the electrostatic energy of the normal spinel structure is lower than the energies of all

inverse configurations for $u > 0.2592$, while the lowest-energy inverse configuration is below the normal structure for $u < 0.2578$. On the other hand, if $Z_A < Z_B$, the electrostatic energy of the normal spinel structure is lower for $u < 0.2550$ and the spinel is inverse for $u > 0.2578$. For u lying between these values, that is, for $0.2578 < u < 0.2592$ (in the $Z_A > Z_B$ case) or $0.2550 < u < 0.2578$ (when $Z_A < Z_B$), the PIE energy differences between different atomic configurations are small and comparable to contributions coming from other, nonelectrostatic types of interactions. Therefore, in these regions the PIE model alone is not sufficient to delineate normal from inverse. However, according to the structure parameters reported in the literature, only a small number of spinels ($\sim 6\%$) are concerns. The PIE model successfully classifies normal versus inverse spinels for $\sim 98\%$ of all other spinel oxides.

■ UNIVERSAL GROUND STATE OF INVERSE A_2BO_4 SPINELS

The configurations of the inverse spinel are represented within the supercell approximation. The parameters a and u are kept fixed, thereby neglecting the local relaxations due to broken cubic symmetry. It was shown in ref 18 that the energy differences between configurations, as obtained from density functional theory (including cell-internal and cell-external strain relaxation), can be recovered remarkably well from the PIE model, at the expense of a single fitting parameter ϵ . We calculate the electrostatic energies of inverse spinels for all 2987 inequivalent inverse configurations with 56 or fewer atoms. In Figure 3a, these 2987 energies are plotted versus configuration number for $Z_A = 3$, $Z_B = 2$, $Z_O = -2$, $a = 8.5$ Å, and $u = 0.262$. The ordered $P4_122$ inverse spinel structure emerges as the structure that has the lowest electrostatic energy. This result does not change after the supercell size is increased to 1512 atoms, which has been proven by the simulated annealing technique. Because at fixed $\lambda = 1$ value the $\Delta E_{\text{PIE}}(\sigma_1, \sigma_2)$ scales as $Z_r^2/a\epsilon$, as discussed previously, this result does not depend on any of the parameters of the model (Z_A , Z_B , a , u , ϵ) as long as $Z_A \neq Z_B$. Therefore, the PIE model identifies the tetragonal $P4_122$ structure as the universal ground-state structure of all spinel oxides known to be inverse ($\lambda = 1$) at $T > 0$. The most stable and the only $\lambda = 0$ structure is, as usual, the $Fd3m$ normal spinel structure.

The physical reasons for the electrostatic preference toward the $P4_122$ structure ($\lambda = 1$) can be appreciated by studying the coordination of the cations occupying the O_h sites. In the spinel structure, each O_h site is coordinated in the second shell by six other O_h sites (see Figure 1a) that form the trigonal antiprism. In the $P4_122$ structure, each octahedral A has two A and four B as second neighbors, and each octahedral B has two B and four A cations as second neighbors (see Figure 1b). Thus, $P4_122$ maximizes the number of A–B pairs in the second shell. This is also true for the next O_h – O_h coordination shell. Since it is electrostatically more favorable to have as many A–B interactions as possible instead of the equivalent number of A–A and B–B for any $Z_A \neq Z_B$, this structure is the electrostatic inverse global minimum. Higher-order O_h – O_h shells contribute much less to the energy and the condition of creating the maximal possible number of A–B pairs in all coordination shells would lead to frustration.

To test the accuracy of the PIE model, we performed the DFT calculations on four spinel oxides that are known to be inverse at high T .² Two of these (Al_2NiO_4 and Ga_2MgO_4) belong to the 3-2 electrostatic family, and the other two (Zn_2SnO_4 and Mg_2VO_4) are 2-4 spinels. Calculations are done

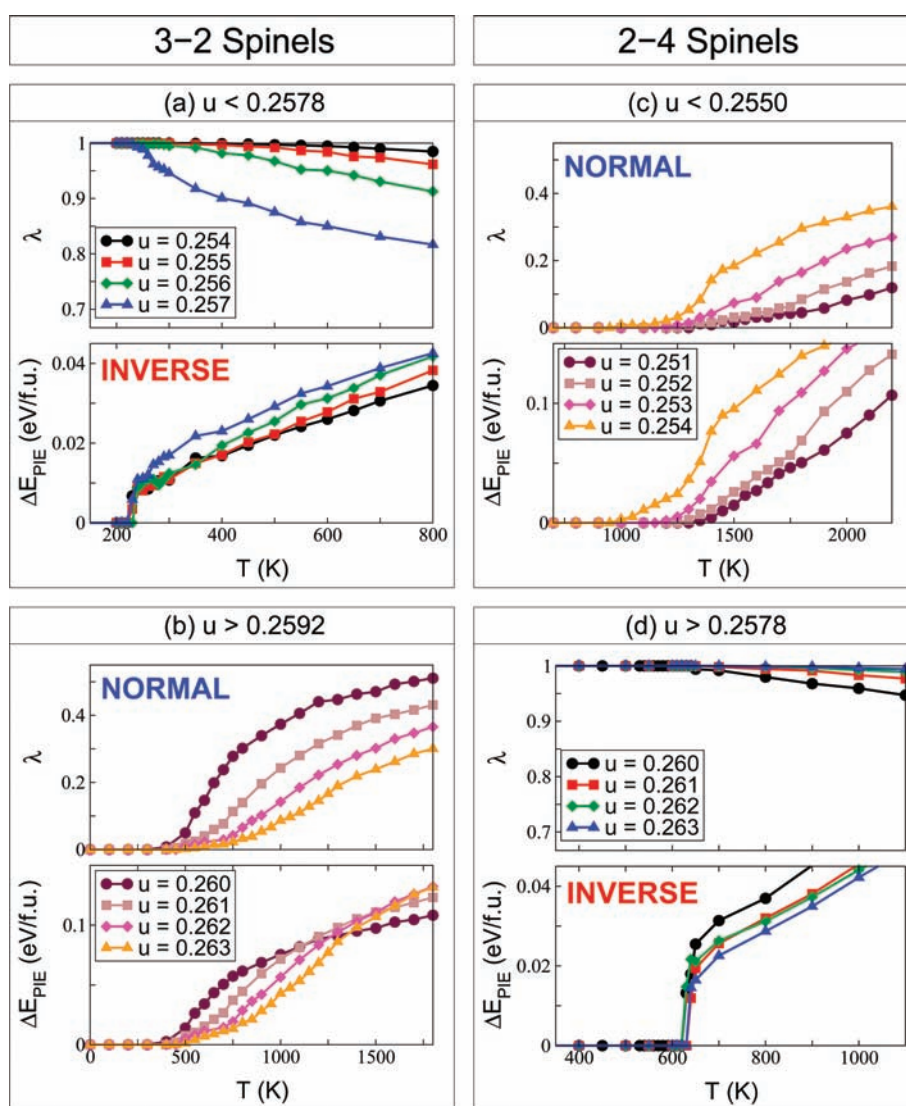


Figure 4. Results of finite temperature Monte Carlo simulations performed with the PIE Hamiltonian. Presented results correspond to both 3-2 (left) and 2-4 (right) spinel oxides. In each case, eight different u values are considered, four of which correspond to the normal (b, c), and four to the inverse (a, d) ground state. During the calculations, the lattice constant was fixed to $a = 8.5 \text{ \AA}$ while $\epsilon = 10$ and $\epsilon = 15$ for the 3-2 and 2-4 spinel oxides, respectively.

on 50 randomly chosen inverse configurations out of 2987 with up to 56 atoms. All DFT calculations are performed with the PBE exchange–correlation functional,²² within the projected augmented wave method²³ as implemented in VASP.²⁴ The density of the Monkhorst–Pack k -point mesh²⁵ is kept constant to the value corresponding to the $6 \times 6 \times 6$ mesh for the 14-atom primitive cell of the normal spinel structure. The plane wave cutoff of 400 eV is used.

The results shown in Figure 3b demonstrate the regression $\Delta E_{\text{DFT}}(\sigma) = 1/\epsilon \Delta E_{\text{PIE}}(\sigma, \epsilon = 1) + \eta$ between PIE and DFT energies computed by taking the $P4_122$ structure as a reference. The value of the lattice constant a , the input parameter to the PIE model, is taken from experiments,^{26–28} whereas in the DFT calculations all lattice vectors and the atomic positions have been relaxed to equilibrium. The fitted value of η is equal to zero in all cases (note the data in Figure 3b are artificially shifted along the y -axes). The results in Figure 3 for the two compounds Ga_2MgO_4 and Zn_2SnO_4 show that (i) the regression is accurate with rather small root-mean-square errors (rms) and (ii) the DFT lowest-

energy configuration is the tetragonal $P4_122$ structure. This proves that the main interactions in these systems are electrostatic in nature. In the case of the other two compounds that contain magnetic atoms (Al_2NiO_4 and Zn_2VO_4), the rms is higher, indicating that magnetic interactions also play a role. Contrary to the result of Palin and Harrison,¹⁵ our DFT calculations show that $P4_122$ is not the ground-state structure for Al_2NiO_4 (it is the ground state in the nonmagnetic calculations). However, one could argue that in this case the ground-state structure is difficult to identify since there are about 20 different inverse configurations that lie in a 70 meV per formula unit (fu) (10 meV/atom) range above the lowest DFT structure. Furthermore, the lowest-energy structure predicted by DFT lies only ~ 60 meV/fu below $P4_122$. This is not the case for Zn_2VO_4 , where the ordered inverse is the lowest-energy structure also in DFT. Despite the disagreement between the PIE model and DFT for the ground-state structure of Al_2NiO_4 , the overall regression of ΔE_{PIE} and ΔE_{DFT} is rather good (for Ga_2MgO_4 almost exact) with the rms error equal or below 4 meV/fu.

There are two important implications of the regression of ΔE_{PIE} and ΔE_{DFT} : (i) to a good approximation, there is a universal scalability between ΔE_{DFT} for different compounds, and (ii) Since 2-4 spinels have approximately up to 2 times bigger ε values than 3-2 spinels [$\varepsilon = 13.6$ (Zn_2SnO_4) and $\varepsilon = 18.5$ (Zn_2VO_4) for the 2-4 cases, while $\varepsilon = 9.8$ (Al_2NiO_4) and $\varepsilon = 11.1$ (Ga_2MgO_4) for the 3-2 spinel oxides], the scaling factor $Z_r^2/a\varepsilon$ is 2–4 times bigger in 2-4 than in 3-2 spinels (if similar lattice constants are assumed). Intuitively, one expects that in the 2-4 spinels electrostatic interactions are more dominant than in 3-2 spinels because of the larger $Z_A - Z_B$. Indeed, for the compounds studied here, the relative energies between two fixed inverse configurations are 2–4 times bigger in 2-4 than in 3-2 spinel oxides. The value of the lattice constant a does not influence considerably this result, since in all spinel oxides a is known to be between 8 and 9 Å.²⁶ A similar electrostatic model, that also uses formal oxidation states as ionic charges and neglects local relaxations, has been shown to reproduce successfully various types of ordering in complex perovskite alloys.³⁰ In the case of spinel oxides our PIE model, in addition to identifying the ordering types, can also be used as an accurate tool in reproducing the universal finite temperature behavior in these materials as shown in the following section.

UNIVERSAL FINITE TEMPERATURE BEHAVIOR IN SPINEL OXIDES

Ordering in inverse spinels has been observed experimentally almost exclusively in 2-4 spinels Mg_2TiO_4 ,^{7–9} Zn_2TiO_4 , and Mn_2TiO_4 ,^{9–11} with the critical temperature $T_c = 933 \pm 20$ K reported for Mg_2TiO_4 .⁸ DFT calculations predict that the T_c values in inverse 2-4 spinels (Zn_2TiO_4 , Mg_2TiO_4 , Zn_2SnO_4 , and Mg_2SnO_4) lie in the range ~ 500 – 1100 K,¹⁴ whereas in inverse 3-2 spinels (Ga_2MgO_4 , In_2MgO_4 , Fe_2MgO_4 , Al_2MgO_4 , and Fe_3O_4) the T_c values are almost an order of magnitude lower and lie in the range ~ 100 – 300 K.^{14,15} These facts may explain the lack of experimental evidence of ordering in 3-2 inverse spinel oxides. Moreover, it is also very well-known experimentally that 2-4 spinel oxides are typically either fully normal ($\lambda = 0$) or fully inverse (ordered or disordered, but with $\lambda = 1$), whereas when dealing with 3-2 spinels, typical samples are disordered-dual with their λ values relatively close but never exactly equal to 0 or 1.

The discussed scaling properties of the PIE relative energies lead to a natural conclusion of universality in the finite temperature behavior in these systems. In order to study the finite temperature behavior in spinel oxides (both normal and inverse), we performed Metropolis Monte Carlo (MC) simulations²⁹ using the PIE Hamiltonian eq 2. The MC method naturally includes the short-range order. We use $a = 8.5$ Å in all cases, while $\varepsilon = 10$ and $\varepsilon = 15$ for 3-2 and 2-4 spinels, respectively. These ε values are representative for the four compounds studied in this work (shown in Figure 3b). We investigated the dependence on the oxygen displacement parameter u , which decides the type of spinel (normal or inverse), by performing MC simulations for different u values for both 3-2 and 2-4 spinels (see Figure 4). A 1512-atom cell is used for this purpose. Further increase in the cell size is verified not to change the final results. Calculations at each temperature are performed with a large number of trial moves ($\sim 10^6$ – 10^7). Each trial move corresponds to a single cation swap that involves both O_h and T_d sites. Results are considered converged if the average energy transfer between the system and the bath is smaller than 0.1 meV for the whole system.

All calculation are performed starting both from the completely random configurations as well as from the corresponding ground states. Characteristic temperatures for the structural transitions are converged to within ± 30 K.³¹

Results of the MC simulations are presented in Figure 4 for inverse 3-2 and 2-4 spinels (panels a and d, respectively) and normal 3-2 and 2-4 (panels b and c, respectively). We show temperature dependence of the average degree of inversion λ as well as the average PIE energy relative to the corresponding normal or inverse ground state. We use average PIE energy and average λ value as indicators of the characteristic temperatures. Both quantities change continuously in cases of continuous disordering, whereas the average energy has a discontinuity in the case of the first-order transition in inverse spinel oxides. In Figure 4, we present results for different u values that lie in the regions of applicability of the PIE model as already discussed. In agreement with the phenomenology presented in Figure 2, the PIE model identifies two different types of structural changes: (i) the first-order ordered-inverse \rightarrow disordered-inverse transition (Figure 4a,d) and (ii) the two continuous disordered-inverse \rightarrow disordered-dual (Figure 4a,d) and normal \rightarrow disordered-dual structural changes (Figure 4b,c). Evidence for the first-order transition is the discontinuity in the average PIE energy that occurs at 230 K for 3-2 spinels and at 620 K for those belonging to the 2-4 family. These values clearly reflect the scaling of the relative PIE energies. Namely, for the parameters used, the relative PIE energies are exactly 2.66 times bigger in 2-4 than in 3-2 spinels. Furthermore, the transition occurs at a constant $\lambda = 1$ where the relative energies between inverse configurations are independent of u (Figure 4a,d). Since the lattice parameters of spinel oxides are more or less all within 1 Å of one another, it follows that the transition temperatures depend mostly on the relative cation charges and ε . For the ε values obtained for compounds shown in Figure 3b, the T_c is about 2–4 times bigger in the studied 2-4 spinels than in 3-2 spinels (in ref 18, we fit even larger $\varepsilon = 13.4$ value for the 3-2 spinel Al_2MgO_4). Just from the scaling, it follows that $T_c = 200$ – 220 K for Ga_2MgO_4 and $T_c = 670$ – 680 K for Zn_2SnO_4 . The second, disordered-inverse \rightarrow disordered-dual continuous change is not independent of the u value since the cost in energy to make a single cation swap between O_h and T_d sites does depend on u . In the case of inverse 3-2 spinels for $u = 0.254$, the degree of inversion starts to deviate appreciably from the $\lambda = 1$ value at ~ 600 K, far above the T_c of the first-order transition. This temperature becomes lower as the u value approaches the borderline for the inverse structure ($u = 0.2578$). For $u = 0.257$, very close to the borderline, the two transitions almost merge. Since in inverse 3-2 spinels the measured u values are typically between 0.255 and 0.257 (see Supplemental Material of ref 18), it is not surprising that in experiments these spinels always occur as disordered-dual. On the other hand, in inverse 2-4 spinels the ordering occurs at higher temperatures (above ~ 700 K), and therefore, they often appear in experiments as fully inverse (in some cases ordered), since typical annealing temperatures go from 500 to 1000 K.⁸ Similarly, in normal spinels (Figure 4b,c), temperatures at which λ starts to deviate from the $\lambda = 0$ value do depend on u as the disordering involves the exchange of cations between O_h and T_d sites. In normal 3-2 spinels (Figure 4b) the energy needed for a single O_h – T_d swap grows as the u value increases, implying the same for the characteristic temperatures. For $u = 0.260$, close to the borderline ($u = 0.2592$) value, the change starts at $T \sim 300$ K, and as the value of u increases to 0.263, it is pushed to $T \sim 450$ K. Again in

2-4 spinels the trend is opposite: the characteristic temperature increases with decreasing u value (direction in which the single O_h-T_d swap becomes more “expensive”) and the change starts occurring at higher temperatures. They start at $T \sim 900$ K for $u = 0.254$ close to the borderline and are pushed to $T \sim 1300$ K for $u = 0.251$. Since typical u values of the normal 2-4 spinels lie in the range 0.239–0.251, this explains why 2-4 spinels occur as fully normal ($\lambda = 0$) in reality.

CONCLUSION

We applied a simple point-ion electrostatic model to the general problem of the structure of spinel oxides. We show that the PIE model provides a universal description of the order–disorder phenomena in these systems. In addition to explaining the normal versus inverse ground-state structural preference, it identifies the tetragonal $P4_122$ structure as the universal ground-state structure of all inverse spinel oxides. Moreover, we show that the PIE model can be extended to finite temperatures, where it provides accurate description of the cation disordering in these systems. Practical value of the model is in its simplicity and its accuracy, as well as its universality across all spinel oxide materials. It has virtually only one free parameter, the dielectric constant ϵ , that can be, for a particular choice of A_2BO_4 spinel, fitted to a small number of ab initio calculations (a and u can be taken from experiments). We show in this work that the PIE model can be used as a reliable tool for predicting the structure of spinel oxides at all temperatures below the melting point.

AUTHOR INFORMATION

Corresponding Author

vladan.stevanovic@nrel.gov

ACKNOWLEDGMENT

This research is supported by the U.S. Department of Energy, Office of Basic Energy Sciences, Division of Materials Sciences and Engineering, Energy Frontier Research Centers, under Award DE-AC36-08GO28308 to NREL. This research used resources of the National Energy Research Scientific Computing Center, which is supported by the Office of Science of the U.S. Department of Energy under Contract DE-AC02-05CH11231 as well as capabilities of the National Renewable Energy Laboratory Computational Sciences Center, which is supported by the Office of Energy Efficiency and Renewable Energy of the U.S. Department of Energy under Contract DE-AC36-08GO28308.

REFERENCES

- (1) Another widely used way of writing the spinel chemical formula is AB_2O_4 . However, following ref 2, we write A_2BO_4 , which is common for spinels with formal cation valencies $Z_A = 2$ and $Z_B = 4$ such as Mg_2TiO_4 .⁸ The main reason for our choice is because the work presented here is part of a larger project that treats all A_2BX_4 compounds (not only spinels) in different structure types, including olivine Fe_2SiO_4 , β - K_2SO_4 , and La_2CuO_4 , for which A_2BX_4 is the generally used notation.
- (2) Zhang, X.; Zunger, A. *Adv. Funct. Mater.* **2010**, *20*, 1944.
- (3) Grimes, N. W. *Phys. Technol.* **1975**, *6*, 22.
- (4) Dekkers, M.; Rijnders, G.; Blank, D. H. A. *Appl. Phys. Lett.* **2007**, *90*, No. 021903.
- (5) Akimoto, J.; Gotoh, Y.; Kawaguchi, K.; Oosawa, Y. *J. Solid State Chem.* **1992**, *96*, 446.

- (6) Yamasaki, Y.; Miyasaka, S.; Kaneko, Y.; He, J. P.; Arima, T.; Tokura, Y. *Phys. Rev. Lett.* **2006**, *96*, No. 207204.
- (7) Delamoye, P.; Michel, A. C. R. *Acad. Sci., Ser. C* **1969**, *269*, 837.
- (8) Wechsler, B. A.; Navrotsky, A. *J. Solid State Chem.* **1984**, *55*, 165.
- (9) Millard, R. L.; Peterson, R. C.; Hunter, B. K. *Am. Mineral.* **1995**, *80*, 885.
- (10) Vincent, H.; Joubert, J.-C.; Durif, A. *Bull. Soc. Chim. Fr.* **1966**, 246.
- (11) Bertaut, E. F.; Vincent, H. *Solid State Commun.* **1968**, *6*, 269.
- (12) Ivanov, V. G.; Abrashev, M. V.; Iliev, M. N.; Gospodinov, M. M.; Meen, J.; Aroyo, M. I. *Phys. Rev. B* **2010**, *82*, No. 024104.
- (13) Seko, A.; Yuge, K.; Oba, F.; Kuwabara, A.; Tanaka, I. *Phys. Rev. B* **2006**, *73*, No. 184117.
- (14) Seko, A.; Oba, F.; Tanaka, I. *Phys. Rev. B* **2010**, *81*, No. 054114.
- (15) Palin, E. J.; Harrison, R. J. *Am. Mineral.* **2007**, *92*, 1334.
- (16) O’Neil, Navrotsky, A. *Am. Mineral.* **1983**, *68*, 181.
- (17) Carpenter, M. A.; Powel, R.; Salje, E. K. H. *Am. Mineral.* **1994**, *79*, 1053.
- (18) Stevanović, V.; d’Avezac, M.; Zunger, A. *Phys. Rev. Lett.* **2010**, *105*, No. 075501.
- (19) Barth, T. F. W.; Posnjak, E. *J. Washington Acad. Sci.* **1931**, *21*, 255.
- (20) Barth, T. F. W.; Posnjak, E. *Z. Kristallogr.* **1932**, *82*, 325.
- (21) Ewald, P. P. *Ann. Phys.* **1921**, *369*, 253–287.
- (22) Perdew, J. P.; Burke, K.; Ernzerhof, M. *Phys. Rev. Lett.* **1996**, *77*, 3865.
- (23) Blöchl, P. E. *Phys. Rev. B* **1994**, *50*, 17953.
- (24) Kresse, G.; Furthmüller, J. *Comput. Mater. Sci.* **1996**, *6*, 15.
- (25) Monkhorst, H. J.; Pack, J. D. *Phys. Rev. B* **1976**, *13*, 5188.
- (26) Hill, R. J.; Craig, J. R.; Gibbs, G. V. *Phys. Chem. Miner.* **1979**, *4*, 317.
- (27) Bergerhoff, G.; Brown, I. in *Crystallographic Databases*; Allen, F. H., Bergerhoff, G., Sievers, R., Eds.; International Union of Crystallography: Chester, U.K., 1987.
- (28) Belsky, A.; Hellenbrandt, M.; Karen, V. L.; Luksch, P. *Acta Crystallogr.* **2002**, *B58*, 364.
- (29) Metropolis, N.; et al. *J. Chem. Phys.* **1953**, *21*, 1087.
- (30) Bellaiche, L.; Vanderbilt, D. *Phys. Rev. Lett.* **1998**, *81*, 1318.
- (31) The predicted temperatures account only for configurational entropy while neglecting other smaller contributions, for example, from vibrational entropy.